ACS APPLIED MATERIALS & INTERFACES

Research Article

www.acsami.org

Fabrication of Microlens Arrays by Localized Hydrolysis in Water Droplet Microreactors

Jun Liu,[†] Meng-Jie Chang,[†] Yong Ai,[†] Hao-Li Zhang,*[,†] and Yong Chen[‡]

[†]State Key Laboratory of Applied Organic Chemistry (SKLAOC), College of Chemistry and Chemical Engineering, Lanzhou University, Lanzhou, Gansu, 730000, China

[‡]Ecole Normale Supérieure, CNRS-ENS-UPMC UMR 8640, 24 rue Lhomond, 75005 Paris, France

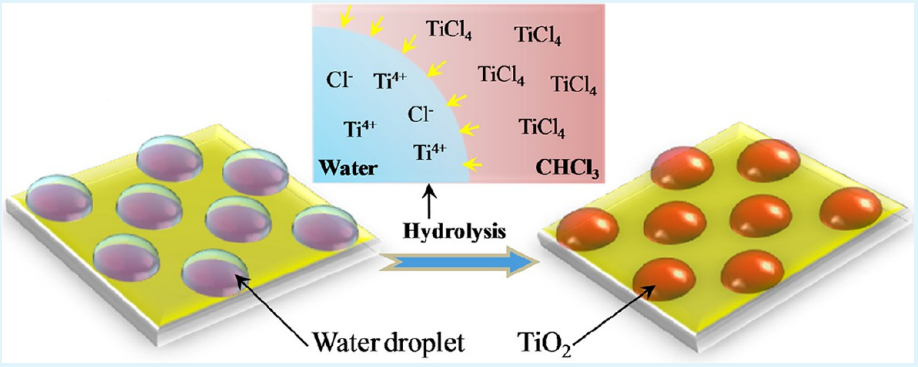

ABSTRACT: We report a facile self-assembly strategy for fabricating TiO_2 microlens arrays by localized hydrolysis of $TiCl_4$ precursor in water droplets. Microcontact printing was used to define hydrophilic areas on a substrate for space resolved hydrolytic reaction. The water droplets served as the templates, reactant, and microreactors. Highly ordered TiO_2 microlens arrays could be produced, which exhibit excellent ability to focus light. Because both size and shape of the final TiO_2 microlens can be controlled by the printed chemical pattern and the precursor concentration, it is possible to define TiO_2 microlens arrays with different imaging properties. This new method shows attractive features of simplicity, low cost, and requires no heating process, hence is suitable for a range of applications.

KEYWORDS: *microlens, droplet, microreactor, pattern, titanium oxide*

INTRODUCTION

This paper describes a self-assembly approach for the fabrication of patterned microlens arrays with well-controlled array structures and lateral dimensions. This method initiates by forming an array of water droplets on a chemically patterned substrate defined by microcontact printing (μCP).[1] The water droplet arrays serve as both template and reactant to allow localized hydrolysis of titanium precursor to take place in the water droplet microreactors, and finally give an array of TiO_2 hemispheres. The structural features of the TiO_2 hemisphere array can be readily controlled by the chemical patterns and the hydrolysis conditions.

Two- and three-dimensional periodic arrays on the scale of the wavelength of light have been applied to fabricate optical devices, including microlens arrays, diffractive optical elements, gratings and photonic crystals.[2−5] Microlens arrays are an important type of miniaturized optical component used in a wide range of applications, such as beam collimators, fiber optic couplers, light homogenizers,[2,6] single molecule bioimaging,[7] assisted formation of protein arrays[8] and efficiency enhancement in optical and electrical devices.[9−11] A variety of methods have been reported to fabricate microlens arrays, mostly involving either photolithography process[12,13] or molding from masters.[2] These microfabrication procedures generally require sophisticated instruments and/or annealing step. Several methods based on self-assembly processes have been developed in recent years, which may offer low cost and easy fabrication process. For example, Hayashi et al. demonstrated that 2D lattices of self-assembled polystyrene beads on glass substrates could be used as arrays of microlens for imaging.[14] Gilchrist et al. also fabricated microlens arrays though assembling SiO_2/polystyrene microspheres.[15] Xia reported the preparation of microsphere array via assembly of polymer microspheres on templates containing cylindrical holes.[16] However, as microspheres are not ideal microlens for imaging, additional heating steps were employed to convert the polymer spheres into hemisphere shape. Besides, the above methods generally produce microlens of polymeric materials, which have relatively low refractive index ($n < 1.6$) and low stability upon thermal or solvent treatments.[17−20] Therefore, for advanced optical or biological applications, it is desirable to fabricate microlens arrays with high refractive index and stable materials.[21,22]

Received: January 8, 2013
Accepted: February 25, 2013
Published: February 25, 2013

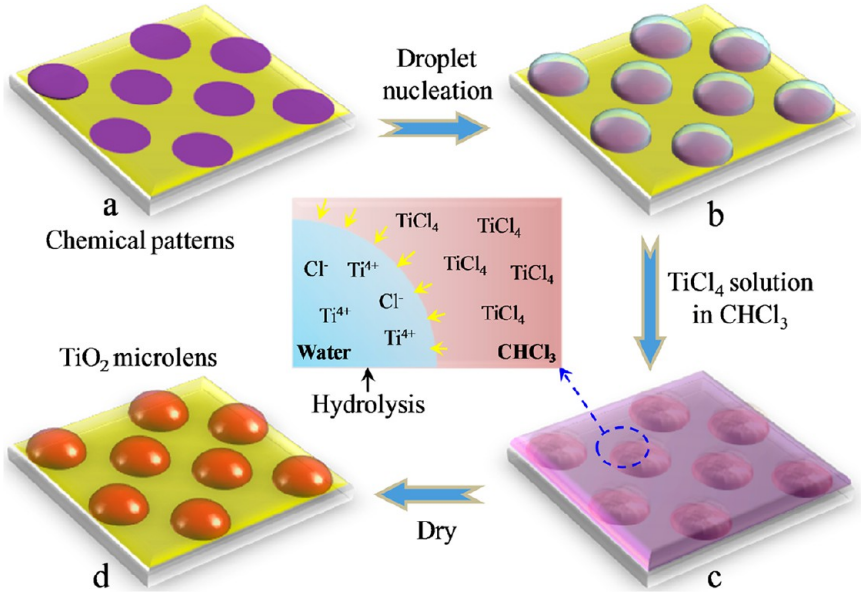

Figure 1. Schematic diagram of the TiO_2 microarrays formation by hydrolysis reaction in water droplets: (a) the hydrophobic/hydrophilic microarray formed by microcontact printing; (b) formation of water droplet arrays; (c) dipping of the substrate into the $TiCl_4/CHCl_3$ solution; (d) solvent evaporation followed by a drying process to give amorphous TiO_2. The graph at the center depicts the diffusion of $TiCl_4$ from the $CHCl_3$ phase into the water droplet and then hydrolysis in the droplet.

Herein, we report a new approach to directly fabricate hemispheric microlens arrays with well-controlled structures through a simple and low-cost process. This method for fabrication of TiO_2 microarrays is based on the localized hydrolysis reaction in water droplet microreactors, which does not require photolithography facility and is conducted at room temperature. TiO_2 is selected as the microlens materials because of its high refractive index ($n > 2.0$) and good chemical stability.[7,23−25] Furthermore, the UV-filtering effect and high biocompatibility of TiO_2 make them suitable for biorelated applications.[26,27]

EXPERIMENTAL METHODS

Materials. Transparent gold coated substrates were prepared by subsequently evaporating chromium (Cr, 2 nm) and gold (Au, 10 nm) on glass substrate by vacuum deposition. 1-octadecanethiol (ODT), 11-mercaptoundecanoic acid (MUA) and $TiCl_4$ were purchased from Aldrich. Microcontact printing of chemical patterns on the gold coated substrates were performed by using poly(dimethylsiloxane) (PDMS) stamps with different topographic features, which were replicated from the SU-8 molds using Dow Coring Sylgard 184 elastomeric kits (Midland, MI).

Fabrication of TiO_2 Microarrays. The gold coated glass substrate with 1×1 cm^2 piece was cleaned under 185 nm UV light for 2 h and rinsed by DI water. The cleaned substrate was printed by a PDMS stamp inked with ODT (1 mM) in ethanol to generate hydrophobic arrays. The patterned substrate was then submerged in a MUA solution (1 mM) in ethanol to form a hydrophobic/hydrophilic alternative pattern. The patterned substrate was put into 70% humid atmosphere to allow water droplets nucleated on the hydrophilic area. Finally, the substrate with water droplets was dipped into a chloroform solution of 1% (v/v) $TiCl_4$ and withdrawn quickly. After that, the substrate was put on a level platform in a clean environment, and the hydrolysis of $TiCl_4$ in the water droplets took place within 5 min at room temperature. The substrates were then dried at room temperature for 48 h to give ordered TiO_2 microarrays. The resulted TiO_2 structures were characterized with scanning electron microscopy (SEM, Hitachi 4800) and atomic force microscopy (AFM, Agilent 5500). Power X-ray diffraction (XRD) measurements were performed on a Shimadzu D6000 X-ray diffractometer with Cu Kα radiation.

RESULTS AND DISCUSSION

The experimental procedure for the fabrication of TiO_2 microarrays is illustrated in Figure 1. First, an alternative hydrophobic/hydrophilic chemical pattern is defined by the μCP and self-assembly techniques of thiol-molecules (ODT and MUA) on gold surface as reported in our previous works (Figure 1a).[1] Water droplets can then be selectively nucleated onto the hydrophilic regions, i.e., MUA coated areas at 70% humid atmosphere (Figure 1b). The substrates coated with water droplets are dipped into the $CHCl_3$ solution of 1% (v/v) $TiCl_4$. After withdrawing, a thin layer of $CHCl_3$ solution can be formed on the substrate (Figure 1c). The $TiCl_4$ in the $CHCl_3$ will soon be extracted into the water phase through the $CHCl_3$/water interface, and start to hydrolyze to give $Ti(OH)_n$. The hydrolysis reaction is accompanied by release of irritating HCl smell.[28] The sample is then slowly dried in dry air at room temperature to avoid cracking of the microdots (Figure 1d). In this process, the water droplets play several roles. First, the water droplets formed on substrate define the positions of the final TiO_2 microdots. Second, water is the reactant for the hydrolysis process. Third, each water droplet serves as a microreactor for the hydrolysis reaction. Because the reaction is confined in the microreactor, the produced $Ti(OH)_n$ structure follows the shape of the droplet, hence is naturally hemispheric.

Figure 2a shows the typical SEM image of the resulted TiO_2 dots. The underplayed chemical pattern consists of round hydrophilic features of 30 μm in diameter. The obtained TiO_2 dots were formed selectively on the hydrophilic areas with uniform size of 30 μm, which is nearly the same as the feature size defined by the PDMS stamp used in the μCP step. Despite the fact that the $CHCl_3$ wets the hydrophobic areas well, the TiO_2 microdots were deposited only in the hydrophilic domains, confirming that the hydrolysis reaction was confined in the water droplets. The morphology of the TiO_2 dots is mainly determined by shape and size of the water droplet template, which can be easily controlled by the chemical patterns. Figure 2b shows that square shaped TiO_2 dots can be

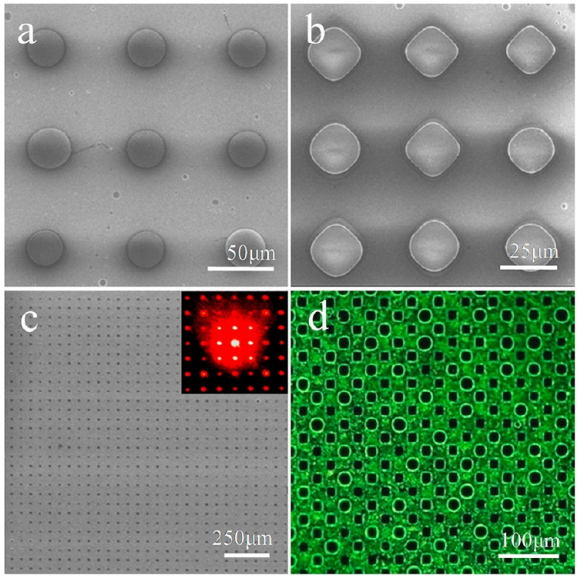

Figure 2. SEM images of the obtained TiO_2 microarrays by the localized reaction in droplets. (a) The stamp feature is 30 μm round shape; (b) the stamp feature is 25 μm squares; (c) large area TiO_2 structures obtained by 16 μm round pattern stamp and the diffraction image when a laser irradiated through the micropattern substrate (inset of c); (d) fluorescent image of the TOPV films formed on the TiO_2 microarrays.

obtained when the underlayed chemical pattern contained 25 μm squares. It is noted that the square TiO_2 microdots have curved corners and the size is slightly smaller than 25 μm, which can be attributed to the shrinking during the drying step. It is possible to prepare other shaped TiO_2 structures by similar method using PDMS stamps with other structural features, such as bar and stripe. As we are interested in microlens for imaging applications, we focused our investigation to the round shape TiO_2 microstructures. Both Figure 2a, b illustrate that the produced TiO_2 dot arrays are highly uniform. Such uniform array can extend to a centimeter scale area. Figure 2c shows a large image of a uniform TiO_2 dot array with literally no defect. Shining a 633 nm laser beam through the microarray produced a regular diffraction pattern (inset of Figure 2c) on the screen, indicating a long-range ordered of the microstructures on the substrate.

As mentioned above, the TiO_2 dot pattern is defined by the hydrophobic/hydrophilic chemical pattern on the substrate. As discussed in our previous works,[1,29] such chemical pattern can also be used to produce a variety of single component or hierarchical structures using a wide range of materials. Because the produced hydrophilic TiO_2 dots only cover the hydrophilic domains, the original hydrophobic/hydrophilic pattern still remains on the substrate after the dot formation process. Therefore, it is possible to selectively deposit another material onto the hydrophobic domains, which may be used as a light blocking or filter layer to increase image contrast. To demonstrate this principle, we have deposited a fluorescent organic dye TOPV[30] onto the hydrophobic areas. Briefly, the water droplets were nucleated on the TiO_2 domains on the substrate, and then the substrate was dipped into a TOPV/$CHCl_3$ solution to form the fluorescent films with order holes like the method described previously.[1] As shown by the fluorescence microscopic image (Figure 2d), the TOPV selectively covers the area outside of the TiO_2 dots. This simple experiment illustrates that more complicated pattern may be formed on the substrates.

Besides using different chemical patterns, the dimension of the TiO_2 microdots could also be tuned by the reaction conditions, such as precursor concentration. To illustrate the effects of the $TiCl_4$ concentration, TiO_2 microdots were prepared from $TiCl_4$ solutions with concentrations of 1, 0.5, and 0.25%, and the substrates were printed with chemical patterns contain 25 μm hydrophilic squares. Figure 3 shows the

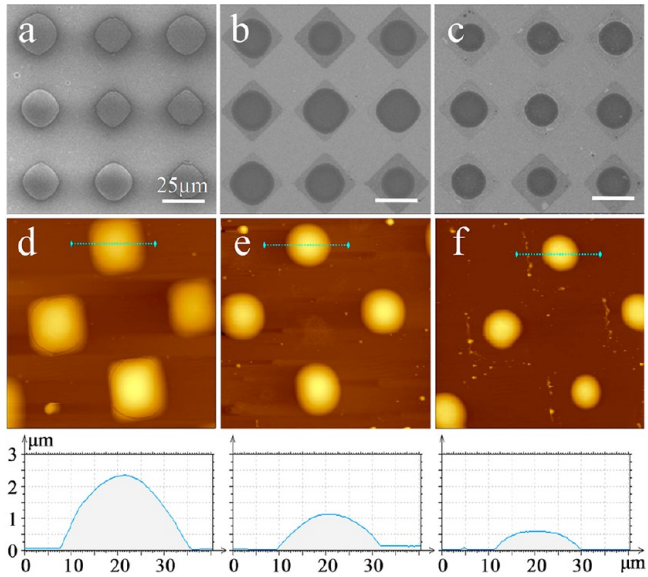

Figure 3. SEM and AFM images of the TiO_2 arrays obtained by the $TiCl_4$ concentration of (a, d) 1, (b, e) 0.5, and (c, f) 0.25%, respectively.

SEM and AFM images of the produced TiO_2 microdots. At 1% $TiCl_4$ concentration, nearly all the hydrophilic squares were covered by TiO_2 and square shaped microdots were produced (Figure 3a). At relative lower concentrations, such as 0.5 and 0.25%, the TiO_2 microdots are all round shape and are smaller than the underlay squares (Figure 3b, c). The size of the microdots decreases slightly with the decreases of the solution concentration. AFM measurements of the TiO_2 microdots (Figure 3d–f) show that the thickness of the microdots decreases with the $TiCl_4$ concentrations. The AFM profiles indicate that the microdots are hemispheric shape with smooth surface morphology, making them good candidate for microlens application. Importantly, the profiles indicate that the dot curvatures decrease with the decrease of $TiCl_4$ concentration, so that their optical properties can be tuned by the $TiCl_4$ concentration. We have also tried to prepare the patterns with much higher (above 5%) or lower concentrations (below 0.1%), but the patterns appeared to have more defects and required more condition optimization to achieve acceptable homogeneity. Under our condition, the most reproducible results appear to be obtained in the concentration range from 0.2 to 2%.

The TiO_2 microdots were obtained by slowly drying process at room temperature, therefore, no crystallization was expected. The amorphous TiO_2 can be converted into crystallized state by calcinations at high temperature. Figure 4 shows the X-ray diffraction (XRD) patterns of the as prepared microarray and the sample calcinated at 450 °C for 3 h in air. The as prepared sample presents no obvious peak, indicating the amorphous

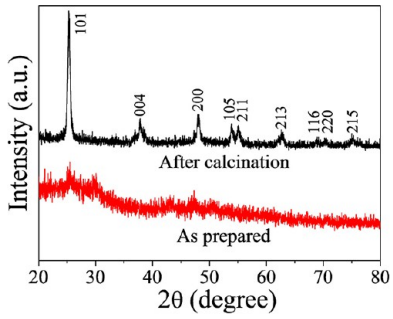

Figure 4. XRD patterns of the as prepared TiO_2 samples and after calcination at 450 °C for 3 h.

structure as expected. In contrast, a series of sharp and intense diffraction peaks of 2θ appeared after calcinations, which are corresponding to the diffraction crystallized face of anatase TiO_2. This result reveals that the amophous TiO_2 was transferred to anatase phase after high temperature calcinations.[31] Unfortunately, calcinations result in the detachment of the microdots from the surface, probably due to the thermal induced deformation of the very thin gold layer. Therefore, we only use the as prepared samples in the following optical characterization.

To demonstrate the possible optical applications of the TiO_2 microarray for light focus, projection experiment was performed with an optical microscope (Nikon Eclipse 80i) as depicted in Figure 5. The TiO_2 microarray was fixed on the sample stage and illuminated with white light through a projection photomask. The distance between the stage and the photomask was set to 20 cm. The substrate deposited with a very thin layer of Cr/Au (2/10 nm) is transparent to light. The

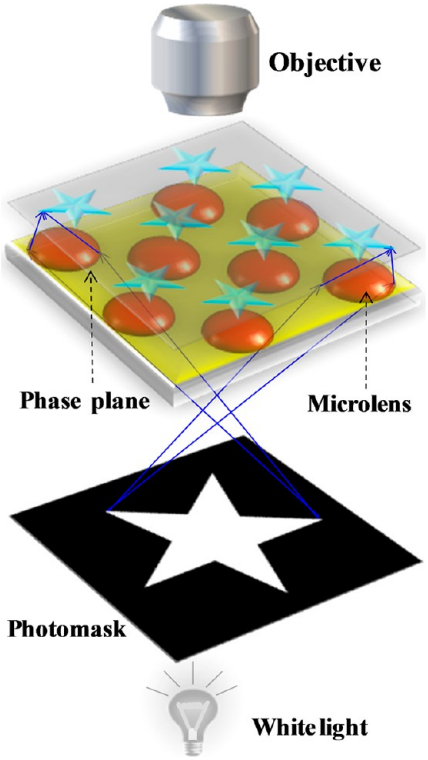

Figure 5. Scheme of the image projection by the microlens and the path of light from the lamp to the phase plane.

photomasks containing different features were made by cutting a black plastic film. The light passing through the photomask was focused by the microlens of the TiO_2 arrays to project miniaturized images of the photomask pattern on a phase plane. The projected image was captured through the camera fixed on the objective lens of the microscope.

The projected image was achieved by the light focus property through the microlens, which results the difference of optical intensity on the phase plane between the image domain and the background. Figure 6a is a typical optical image of the pentagram after projection through an array with 25 μm diameter microlens. It is clear observed that the image possesses the same geometry with the pattern geometry of the photomask. The projected images in the entire substrate by each lens have nearly the same size and resolution, indicating the high uniformity of the optical properties of the microlens arrays. The distance between each adjacent vertex in the pentagram mask is 13 mm, which distance in the generated image is around 12.5 μm. Thus, the reduction archived by this microlens is above 1000 times, which is similar to the reduction ability of the microlens produced by the resist flow method.[12] Taking advantage of the difference in grayscale, the projected image could be mapped with a 3D profile (Figure 6b), which suggests that the image quality is highly uniform. Similarly, other patterns could also be projected by this microlens arrays by changing the patterns on the photomasks. For example, cross patterns were clearly imaged with good contrast (Figure 6c). The Figure 6a–c clearly indicates that the microlens array has a strong focusing capability to white light.

The optical properties (e.g., focal length) of the microlenses were mainly determined by the size and curvatures of the hemisphere. To demonstrate the feasible control of the optical properties by the sizes of the microlens, arrays with feature sizes of 25, 50, and 60 μm were prepared with the same $TiCl_4$ concentration of 1% (Figure 6d). All the arrays show good imaging quality. When a photomask with line width of 2 mm was used, the widths of the projected images were 1.8, 4.5, and 6.1 μm for the 25, 50, and 60 μm microlens, respectively. The reduction time decreases with the increase of the microlens diameter, which is attributed to the smaller curvature with the larger diameter microlens. Furthermore, these microlens arrays are stable in air for several weeks without degradation of the imaging capability.

CONCLUSION

We have demonstrated a simple and highly efficient method to produce TiO_2 microlens arrays by controlled hydrolysis in water droplet microreactors. In comparison with the previous patterning process, the new method reported herein presents several attractive features. First, the size, shape and filling density of the microlens array could be easily tuned by the chemical patterns and the hydrolysis conditions. Second, the water droplets serve as the template for the microlens formation so that ideal hemispheric shape can be readily obtained. Third, no heating procedure is required in the whole process, so that this strategy may be applied to wide range of substrates and materials. Therefore, it is believed that this facile method could find wide applications in high-performance optoelectronic devices and biosensors.

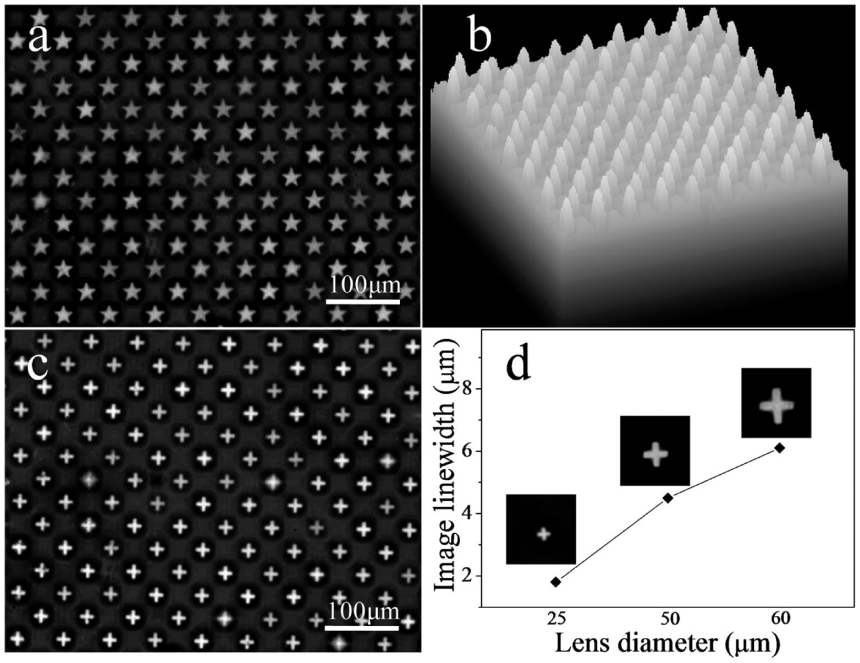

Figure 6. Grayscale optical images of photomask projected by the microlens. (a, c) Optical projected images by the photomask with pentangle or cross patterns through the microlens of 25 μm; (b) 3D plot of the optical intensity of Figure 6a by software of ImageJ; (d) images projected by the microlens with diameter of 25, 50, and 60 μm with the photomask of crosses with 2 mm width.

AUTHOR INFORMATION

Corresponding Author

*E-mail: Haoli.zhang@lzu.edu.cn. Tel. & Fax: +86 931 8912365.

Author Contributions

All authors have given approval to the final version of the manuscript.

Notes

The authors declare no competing financial interest.

ACKNOWLEDGMENTS

This work is supported by National Basic Research Program of China (973 Program) 2012CB933102, National Natural Science Foundation of China (NSFC 21233001, 21190034, 21073079, J1103307), Specialized Research Fund for the Doctoral Program of Higher Education (SRFDP 20110211130001), the Fundamental Research Funds for the Central Universities, and 111 Project.

REFERENCES

(1) Zhang, L.; Si, H. Y.; Zhang, H. L. *J. Mater. Chem.* **2008**, *18*, 2660−2665.
(2) Stevensa, R.; Miyashita, T. *The Imaging Science Journal* **2010**, *58*, 202−212.
(3) Gonzalez-Urbina, L.; Baert, K.; Kolaric, B.; Perez-Moreno, J.; Clays, K. *Chem. Rev.* **2012**, *112*, 2268−2285.
(4) Hatton, B.; Mishchenko, L.; Davis, S.; Sandhagec, K. H.; Aizenberg, J. *Proc. Natl. Acad. Sci. U.S.A.* **2010**, *107*, 10354−10359.
(5) Zhang, J.; Li, Y.; Zhang, X.; Yang, B. *Adv. Mater.* **2010**, *22*, 4249−4269.
(6) Mogi, T.; Hatakeyama, K.; Taguchi, T.; Wake, H.; Tanaami, T.; Hosokawa, M.; Tanaka, T.; Matsunaga, T. *Biosens. Bioelectron.* **2011**, *26*, 1942−1946.
(7) Schwartz, J. J.; Stavrakis, S.; Quake, S. R. *Nat. Nanotechnol.* **2009**, *5*, 127−132.
(8) Zhang, F.; Gates, R. J.; Smentkowski, V. S.; Natarajan, S.; Gale, B. K.; Watt, R. K.; Asplund, M. C.; Linford, M. R. *J. Am. Chem. Soc.* **2007**, *129*, 9252−9253.
(9) Wrzesniewski, E.; Eom, S. H.; Cao, W.; Hammond, W. T.; Lee, S.; Douglas, E. P.; Xue, J. *Small* **2012**, *8*, 2647−2651.
(10) Thomschke, M.; Reineke, S.; Lussem, B.; Leo, K. *Nano Lett.* **2012**, *12*, 424−428.
(11) H. J. Peng, Y. L. H.; Qiu, C. F.; Wong, M.; Kwok, H. S. *SID Symp. Dig. Tech. Papers* **2004**, *35*, 158−161.
(12) Wu, H. K.; Odom, T. W.; Whitesides, G. M. *Anal. Chem.* **2002**, *74*, 3267−3273.
(13) Li, F.; Chen, S.; Luo, H.; Zhou, Y.; Lai, J.; Gao, Y. *Opt. Laser Technol.* **2012**, *44*, 1054−1059.
(14) Hayashi, S.; Kumamoto, Y.; Suzuki, T.; Hirai, T. *J. Colloid Interface Sci.* **1991**, *144*, 538−547.
(15) Kumnorkaew, P.; Ee, Y.-K.; Tansu, N.; Gilchrist, J. F. *Langmuir* **2008**, *24*, 12150−12157.
(16) Lu, Y.; Yin, Y. D.; Xia, Y. N. *Adv. Mater.* **2001**, *13*, 34−37.
(17) Kang, D.; Pang, C.; Kim, S. M.; Cho, H. S.; Um, H. S.; Choi, Y. W.; Suh, K. Y. *Adv. Mater.* **2012**, *24*, 1709−1715.
(18) Wu, M. H.; Whitesides, G. M. *J. Micromech. Microeng.* **2002**, *12*, 747−758.
(19) Ottevaere, H.; Cox, R.; Herzig, H. P.; Miyashita, T.; Naessens, K.; Taghizadeh, M.; Völkel, R.; Woo, H. J.; Thienpont, H. *J. Opt. A: Pure Appl. Opt.* **2006**, *8*, S407−S429.
(20) Chan, E. P.; Crosby, A. J. *Adv. Mater.* **2006**, *18*, 3238−3242.
(21) Lee, K.; Wagermaier, W.; Masic, A.; Kommareddy, K. P.; Bennet, M.; Manjubala, I.; Lee, S. W.; Park, S. B.; Colfen, H.; Fratzl, P. *Nat. Commun.* **2012**, *3*, 1−7.
(22) Aizenberg, J.; Muller, D. A.; Grazul, J. L.; Hamann, D. R. *Science* **2003**, *299*, 1025−1028.
(23) Zhang, M.; Lin, G.; Dong, C.; Wen, L. *Surf. Coat. Technol.* **2007**, *201*, 7252−7258.
(24) Chen, X. B.; Mao, S. S. *Chem. Rev.* **2007**, *107*, 2891−2959.
(25) Yang, S.; Ford, J.; Ruengruglikit, C.; Huang, Q.; Aizenberg, J. *J. Mater. Chem.* **2005**, *15*, 4200−4202.
(26) Danzebrink, R.; Aegerter, M. A. *Thin Solid Films* **2001**, *392*, 223−225.

(27) Mudanyali O.; McLeod E.; Luo W.; Greenbaum A.; F.Coskun A.; Hennequin Y.; Allier C. P.; Ozcan A. *Nat. Photonics* **2013**, *7*, DOI: 10.1038/nphoton.2012.1337.
(28) Li, X.; Zhang, L.; Wang, Y.; Yang, X.; Zhao, N.; Zhang, X.; Xu, J. *J. Am. Chem. Soc.* **2011**, *133*, 3736−3739.
(29) Chang, M. J.; Ai, Y.; Zhang, L.; Gao, F.; Zhang, H. L. *J. Mater. Chem.* **2012**, *22*, 7704−7707.
(30) Gao, F.; Liao, Q.; Xu, Z. Z.; Yue, Y. H.; Wang, Q.; Zhang, H. L.; Fu, H. B. *Angew. Chem., Int. Ed.* **2010**, *49*, 732−735.
(31) Zhao, X.; Jin, W.; Cai, J.; Ye, J.; Li, Z.; Ma, Y.; Xie, J.; Qi, L. *Adv. Funct. Mater.* **2011**, *21*, 3554−3563.